Enhanced optical near field from a bowtie aperture

Eric X. Jin and Xianfan Xu[a)]
School of Mechanical Engineering, Purdue University, West Lafayette, Indiana 47906

(Received 3 November 2005; accepted 28 February 2006; published online 11 April 2006)

The enhanced optical near field from a bowtie aperture in an aluminum film is experimentally demonstrated using near-field scanning optical microscopy. The full width half magnitude near-field optical spot is determined to be about 65×34 nm^2 by 458 nm argon ion laser illumination, which is seven times smaller than those obtained from square and rectangular apertures of the same opening area. Light concentration and transmission enhancement of bowtie apertures promise a highly efficient nanoscale light source for near-field optical applications. © *2006 American Institute of Physics*. [DOI: 10.1063/1.2194013]

The ability to confine light to a nanometer-scale spot of high intensity is of great interest to the study of light interaction with biological materials[1,2] and nanostructures,[3,4] as well as potential applications such as high density data storage[5] and nanolithography.[6,7] A sharp metal tip can result in a strongly enhanced field at its apex using either an asymmetrical metal tip[2] or on-axis illumination.[8] Squeezing light through a nanometer-sized aperture in an opaque screen, on the other hand, offers a convenient way to achieve nanometer-scale light source. However, if not properly designed, the aperture experiences extremely low light transmission[9] because of the waveguide cutoff effect. The enhancement of optical transmission through subwavelength apertures has been recently demonstrated using a hole array,[10] a single hole surrounded by periodic structures[11] via the excitation of surface plasmon polaritons (SPPs), scatterer-formed aperture[12] via localized surface plasmon (LSP), and ridge apertures[13–17] via waveguide propagation mode. In an earlier work, computational results for bowtie apertures showed that potentially they can provide a confined nanometer-scale light spot and high intensity benefiting from the specially designed geometry.[18]

A bowtie aperture is the complement of a bowtie antenna as shown in Fig. 1(a). Both of these consist of two arms and a small gap formed by two sharp tips pointing to each other. The bowtie antenna was proposed in the microwave regime as an efficient near-field probe[19] and was recently configured for applications at optical frequencies.[4,20] Radiation enhancement of the bowtie antennas was demonstrated using the method of photoluminescence of single quantum emitters[4] and two-photon excited photoluminescence of noble metals[20] in order to shift the bowtie radiation frequency from the excitation frequency. A bowtie aperture, on the other hand, has the advantage of blocking the background light; therefore it is best suited in the confinement of incident light with long cutoff wavelength, which is desirable for high density near-field recording, high throughput nanolithography, or other high efficiency near-field optical applications.

In this letter, we provide experimental evidence of the enhanced nanoscale optical near field from a bowtie aperture fabricated in an aluminum film. The transmitted light through the bowtie aperture and regular apertures (square and rectangular) of the same area for the opening is measured using specially designed near-field scanning optical microscopy[21] (NSOM) with a sub-50-nm aperture probe. The bowtie aperture results in a substantially smaller near-field light spot than the common apertures while having transmission efficiency five orders of magnitude higher than the smallest regular nanoaperture designed to produce a near-field spot of comparable size. Using finite difference time domain (FDTD) calculations, the enhanced nanoscale optical transmission through the bowtie aperture is explained as the result of the greatly induced electric fields at its tips coupled through the propagating waveguide mode in the gap.

The bowtie aperture for 458 nm wavelength argon ion laser illumination is designed using FDTD calculations, following the procedures outlined in Ref. 22. Focused ion beam (FIB) milling is used to fabricate the bowtie aperture and square or rectangular apertures in an aluminum thin film on a quartz substrate. Aluminum film is selected because of its small skin depth (6.5 nm at 458 nm illumination) and high reflectivity (0.92 at normal incidence). The thickness of aluminum film was chosen to be 150 nm, which is sufficiently thick to block the light other than that through the apertures. The apertures were made in a 2×2 array pattern for the purpose of comparison as shown in the scanning electron microscopy (SEM) image in Fig. 1(b). The separations between these apertures are large enough (more than 1.2 μm both in the x and y directions) so that the optical near-field interferences are negligible. The bowtie aperture has an outline of about 216×248 nm^2 and a tip radius of 45 nm. The minimum gap spacing between the two tips is 33 nm. It is limited by the finite ion beam size and the beam tail effect. A

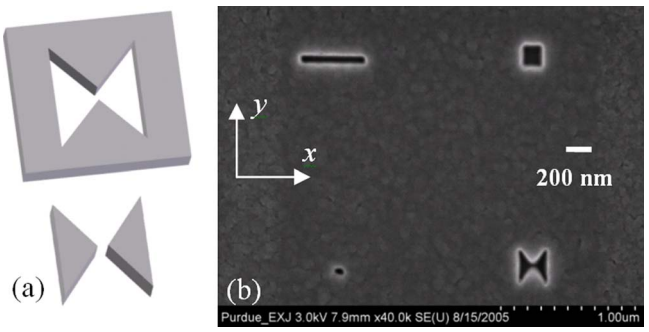

FIG. 1. (Color online) (a) Schematics of bowtie aperture (top) and bowtie antenna (bottom). The gray areas represent metal film. (b) SEM image of bowtie aperture and comparable regular apertures fabricated in 150 nm aluminum on quartz substrate.

a)Electronic mail: xxu@ecn.purdue.edu

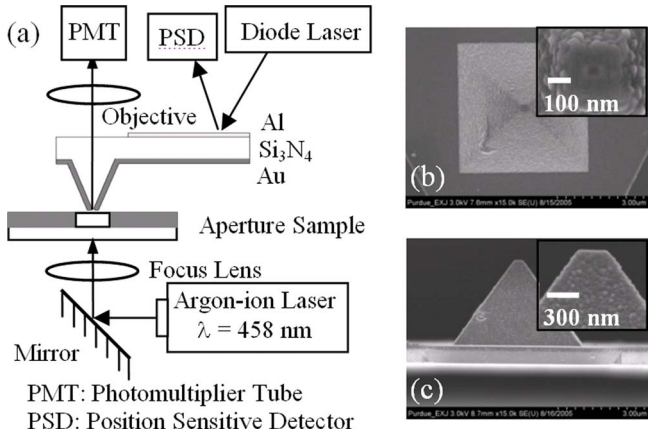

FIG. 2. (Color online) (a) Schematic of the homebuilt near-field scanning optical microscopy (NSOM) system using the cantilevered silicon nitride aperture probe. (b) Top view and (c) side view of the NSOM probe. The insets show that the probe has a flat end of 257×257 nm^2 in size with a 45×45 nm^2 silicon nitride core surrounded by aluminum.

small rectangular nanoaperture [lower left in Fig. 1(b)] of 40×36 nm^2 is made to have about the same area as the gap region between the tips of the bowtie aperture. The square and the large rectangular apertures in the upper half in Fig. 1(b) are about 160×160 nm^2 and 450×60 nm^2, respectively, approximately the same opening area as that of the bowtie aperture shown in the same figure.

To investigate the optical near field of these apertures, an illumination-collection-type NSOM system using cantilevered aperture probe as the optical near-field collector is developed and schematized in Fig. 2(a). FIB is used to make the aperture on the probe. This special aperture probe used for the following NSOM measurement has an opening of 45×45 nm^2 surrounded by aluminum as shown in Figs. 2(b) and 2(c). The overall size of the probe end is 257×257 nm^2 as measured from the side of the probe. The aperture sample is illuminated by an argon ion laser beam (1.2 mW at 458 nm wavelength) from the quartz substrate side. The laser beam is focused on the aperture array and polarized in the y direction across the gap of the bowtie aperture. The transmitted light through the apertures is collected by the probe and directed into a photomultiplier tube (PMT) placed in the far field. A NSOM image is obtained by raster scanning the aperture sample and recording the optical signal from the PMT by photon counting. The soft contact between the probe and sample surface is achieved by maintaining a small and constant normal force based on the feedback of diode laser beam deflected on the cantilever. It should be noted that sub-100-nm optical resolutions can be routinely achieved using our NSOM system and the cantilevered NSOM probes are more durable and easier to handle than commercial tapered fiber probes.

The 2×2 aperture array as displayed in Fig. 1(b) is scanned and the raw data of a two-dimensional (2D) NSOM image is shown in Fig. 3(a). Since the flat end of the probe is larger than all the apertures, it is not inside the apertures during the scanning. Therefore, the NSOM image can be considered as the in-plane electric field intensity profile[23] obtained at the constant height mode with zero distance away from the exit plane of the apertures. It can be seen that the collected intensity is dominated by the transmitted light through the apertures. The intensity profiles along the dotted lines indicated in Fig. 3(a) are plotted in Figs. 3(b) and 3(c).

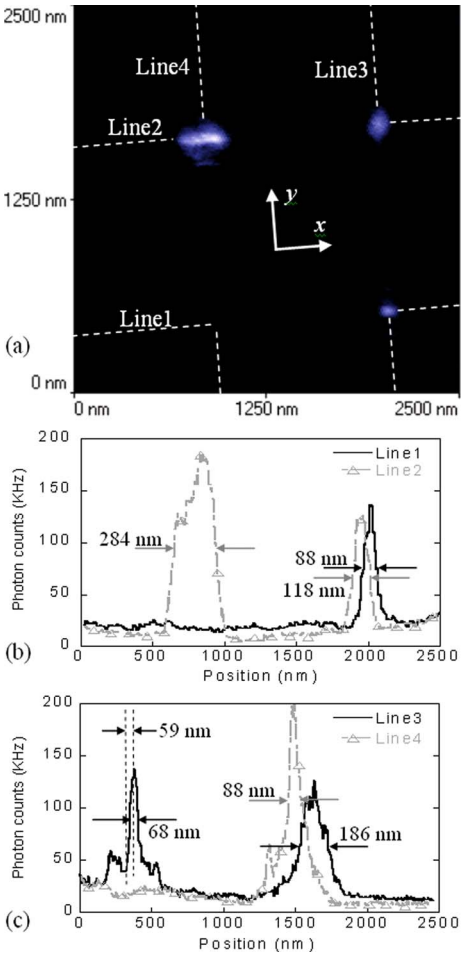

FIG. 3. (Color online) (a) NSOM image of the 2×2 aperture array shown in Fig. 1(b) taken with a 458 nm incident laser polarized in the y direction. The near-field optical profiles of these apertures are displayed in line scans along (b) line 1 and line 2 and (c) line 3 and line 4. The FWHM of the light spots and the edge resolution of the probe is indicated in the plots.

The full width at half magnitude (FWHM) of the transmitted light spots are measured as 88×68 nm^2, 118×186 nm^2, and 284×88 nm^2 for the bowtie, square, and large rectangular apertures, respectively. The smallest aperture in the array is designed to produce a light spot comparable to that obtained by the bowtie aperture, but there is no measurable light signal coming out of it, indicating its expected low transmission. The light spot from the bowtie aperture is much smaller than the overall size of the bowtie aperture. Considering the symmetries of the bowtie aperture and the NSOM light spot, the near-field light through the bowtie aperture has to be localized in the central gap between the bowtie tips instead of coming out of the side arms, which demonstrates the near-field collimation function of bowtie aperture.[18] Two small peaks are found in the line scan profile along the y direction [see line 3 in Fig. 3(c)], but no such feature is found along the x direction. The separation between these two peaks is about 290 nm, larger than the size of the bowtie aperture, meaning they are located on the metal surface. This possibly indicates the excitation of the localized surface plasmon mode with short decay length.

Due to the finite size of aperture probe, the NSOM light spot essentially represents the convolution of the scanning probe transfer function with the actual transmitted light signal through the sample aperture. The characteristic size of

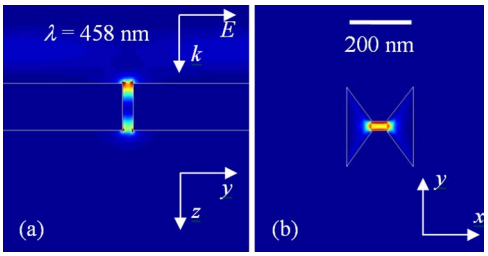

FIG. 4. (Color online) Electric field intensity distribution (a) in the *yz* plane cut through the middle of the tips and (b) in the *xy* plane across the exit plane of the bowtie aperture obtained by FDTD calculation.

the actual light spot $FWHM_{act}$ can be estimated by performing the deconvolution calculation to the first order approximation[24] as

$$(FWHM_{act})^2 = (FWHM_{NSOM})^2 - (RES_{probe})^2, \quad (1)$$

where $FWHM_{NSOM}$ is the measured FWHM of the NSOM light spot and RES_{probe} is the edge resolution of the probe, which is measured to be 59 nm (approximately the sum of the aperture size of 45 nm and twice the skin depth of aluminum of 6.5 nm at the 458 nm wavelength). Using Eq. (1), the actual light spot size from individual apertures can therefore be calculated from the measured NSOM spot size, which results in 65×34 nm^2, 102×176 nm^2, and 278×65 nm^2 for the bowtie, square, and large rectangular apertures, respectively. The comparable square and rectangular apertures therefore have the deconvoluted light spots about seven times larger than that of the bowtie aperture. In addition, the peak PMT signals of the transmitted light through the square, rectangular and bowtie apertures, accounting for the finite size of the probe, are 72 000, 115 000, and 136 000 counts/s, respectively. The incident laser counts over an area equal to the probe opening area are estimated to be about 130 000 counts/s. The bowtie aperture therefore has a transmission efficiency about unity.

One can obtain a smaller output light spot from a regular aperture by reducing its size. However, the calculated transmission efficiency of a square aperture of 40×40 nm^2 is about 10^{-5}, as expected from Bethe's small aperture theory.[9] The bowtie aperture, on the other hand, has the computed transmission efficiency near unity, which is consistent with the experimental result discussed above. Bowtie aperture is therefore able to achieve the optical transmission five orders of magnitude higher than that of the comparable 40 nm square aperture, while still providing a nanoscale near-field light spot.

The light propagation through the bowtie aperture is computed using FDTD to illustrate the enhanced transmission brought by the bowtie structure. Figures 4(a) and 4(b) show the calculated electric field intensity distribution in the *yz* plane cut through the middle of the tips and in the *xy* plane across the exit plane of the bowtie aperture, respectively. It is seen that the bowtie tips induce enhanced fields at their vicinity, similar to what occurs in sharp metal tips used for the apertureless NSOM experiments.[2,8] The fields in the entrance and exit planes are coupled through the propagating waveguide mode localized in the bowtie gap, resulting in enhanced transmission with a nanometer-sized near-field light spot. It is believed that the transmission in a bowtie aperture can be further improved by the resonant excitation of the coupled LSP modes of the two bowtie tips.[18,20] This will require choosing a noble metal as the film material; optimizing the film thickness, the overall size of the aperture, the radius of the tips and the distance between the tips, and using high resolution nanofabrication tools to fabricate the desired aperture.

In summary, enhanced optical transmission at the nanometer scale through a bowtie aperture has been experimentally demonstrated by performing near-field measurements using an aperture NSOM system. The near-field light spot through the bowtie aperture has a FWHM size of 65×34 nm^2, which is seven times smaller than those obtained by the square and rectangular apertures of the same opening area. The light spot is localized in the gap between the tips showing the near-field collimation function of the bowtie aperture. The nanoscale light transmission enhancement of the bowtie aperture promises a convenient and highly efficient nanometric light source for near-field optical applications.

The financial supports to this work by the Office of Naval Research and the National Science Foundation are gratefully acknowledged. Fabrications of aperture sample and aperture probe by FIB machining were carried out in the Center for Microanalysis of Materials, University of Illinois, which is partially supported by the (U.S.) Department of Energy under Grant No. DEFG02-91-ER45439.

[1] E. Betzig and R. J. Chichester, Science **262**, 1422 (1993).
[2] E. J. Sanchez, L. Novotny, and X. S. Xie, Phys. Rev. Lett. **82**, 4014 (1999).
[3] A. Hartschuh, E. J. Sanchez, X. S. Xie, and L. Novotny, Phys. Rev. Lett. **90**, 095503 (2003).
[4] J. N. Farahani, D. W. Pohl, H.-J. Eisler, and B. Hecht, Phys. Rev. Lett. **95**, 017402 (2005).
[5] E. Betzig, J. K. Trautman, R. Wolfe, E. M. Gyorgy, P. L. Finn, M. H. Kryder, and C.-H. Chang, Appl. Phys. Lett. **61**, 142 (1992).
[6] I. I. Smolyaninov, D. L. Mazzoni, and C. C. Davis, Appl. Phys. Lett. **67**, 3859 (1995).
[7] Z. W. Liu, Q. H. Wei, and X. Zhang, Nano Lett. **5**, 957 (2005).
[8] L. Novotny, R. X. Bian, and X. S. Xie, Ultramicroscopy **71**, 21 (1998).
[9] H. Bethe, Phys. Rev. **66**, 163 (1944).
[10] T. W. Ebbesen, H. J. Lezec, H. F. Ghaemi, T. Thio, and P. A. Wolff, Nature (London) **391**, 667 (1998).
[11] H. J. Lezec, A. Degiron, E. Devaux, R. A. Linke, L. Martin-Moreno, F. J. Garcia-vidal, and T. W. Ebbesen, Science **107**, 820 (2002).
[12] K. Tanaka, H. Hosaka, K. Itao, M. Oumi, T. Niwa, T. Miyatani, Y. Mitsuoka, K. Nakajima, and T. Ohkubo, Appl. Phys. Lett. **86**, 1083 (2003).
[13] X. Shi, L. Hesselink, and R. L. Thornton, Opt. Lett. **28**, 1320 (2003).
[14] A. V. Itagi, D. D. Stancil, J. A. Bain, and T. E. Schlesinger, Appl. Phys. Lett. **83**, 4474 (2003).
[15] E. X. Jin and X. Xu, Jpn. J. Appl. Phys., Part 1 **43**, 407 (2004).
[16] J. Matteo, D. Fromm, Y. Yuen, P. Schuck, W. Moerner, and L. Hesselink, Appl. Phys. Lett. **85**, 648 (2004).
[17] K. Şendur, C. Peng, and W. Challener, Phys. Rev. Lett. **94**, 043901 (2005).
[18] E. X. Jin and X. Xu, Appl. Phys. Lett. **86**, 111106 (2005).
[19] R. D. Grober, R. J. Schoelkopf, and D. E. Prober, Appl. Phys. Lett. **70**, 1354 (1997).
[20] P. J. Schuck, D. P. Fromm, A. Sundaramurthy, G. S. Kino, and W. E. Moerner, Phys. Rev. Lett. **94**, 017402 (2005).
[21] D. Courjon and C. Bainier, Rep. Prog. Phys. **57**, 989 (1994).
[22] X. Xu, E. X. Jin, S. M. Uppuluri, and L. Wang, J. Phys.: Conference Series (to be published). (2005).
[23] L. Yin, V. K. Vlasko-Vlasov, A. Rydh, J. Pearson, U. Welp, S.-H. Chang, S. K. Gray, G. C. Schatz, D. E. Brown, and C. W. Kimball, Appl. Phys. Lett. **85**, 467 (2004).
[24] J. M. Imhof, E.-S. Kwak, and D. A. Vanden Bout, Rev. Sci. Instrum. **74**, 2424 (2003).